

UDC 621.929.2/.9  
DOI 10.12737/1558

## **DEVELOPMENT OF MATHEMATICAL MODELS OF CENTRIFUGAL MIXING UNITS OF NEW DESIGN FOR THE PRODUCTION OF DRY COMBINED FOOD PRODUCTS**

**V. N. Ivanets and D. M. Borodulin**

Kemerovo Institute of Food Science and Technology,  
bul'v. Stroitelei 47, Kemerovo, 650056 Russia  
phone: +7(3842) 39-68-42, e-mail: Borodulin\_dmitri@list.ru

(Received January 17, 2013; Accepted in revised form February 25, 2013)

---

**Abstract:** A method of modeling the continuous process of the mixing of bulk materials on the basis of cybernetic analysis with some elements of automatic control theory (ACT) [6, 9] has been considered. In this case, a mixing unit (MU) is represented in the form of a dynamic system, which is characterized by the known topology of the motion of material flows and subjected to various external disturbances.

The two developed mathematical models allow us to determine the degree of the smoothening of input material flow fluctuations from volumetric dosers by the mixers incorporated into a MU. The obtained numerical values of smoothability indicate that it is reasonable to equip the studied mixers of new design with volumetric dosers. This allows us to meet the requirements to MUs from both the engineering and economical viewpoints.

**Key words:** centrifugal mixer, time-and-frequency analysis, bulk materials, combined food products, modeling, cybernetic analysis

---

### **INTRODUCTION**

The contemporary state of the market of food industry equipment is characterized by a considerable increase in the demand for machines and apparatuses that allow the production of high-quality food products of increased nutritional value (enriched with vitamins and biologically essential components) at low expenditures. In particular, the population should have new combined food products that compensate the deficiency of different food components and micronutrients in its ration due to considerable ecological disturbances in different regions of Russia and other countries.

Since the content of many food additives in the major product is small (1% and lower), the key problem consists in their uniform distribution over the entire volume. Using the results of studies, it has been revealed that continuous centrifugal mixers (CCMs) [2, 5] characterized by a high intensity of mixing due to the targeted organization of the motion of thin disperse layers are most promising for the solution of this problem. Centrifugal mixers enable the production of good-quality mixtures at a component ratio of 1:100 [2]. However, a single CCM is usually insufficient at higher ratios. In this connection, we propose to incorporate two serially arranged centrifugal mixers with a good smoothability into a single MU. In this case, it is possible to use volumetric dosers with certain advantages (high material feed rate, small dimensions,

low cost and maintenance expenditures) for the preparation of mixtures with high ratios of mixed components. For this reason, the objective of our work is to compare the operational efficiencies of two centrifugal MU of new design (differ from each other by the set of equipment incorporated in them), in which it is possible to obtain dry combined food products with a high ratio of mixed components, using cybernetic analysis and some ACT elements [6, 7, 9].

When studying the operation of certain mixing equipment, we artificially imposed a disturbance of one or another kind onto the input feed flow and then analyzed its consequences at the output of an apparatus (plotted a response curve) [10]. The function determined from the given curve for the residence time distribution of particles in centrifugal mixers was used in combination with the accepted flow pattern of mixed materials in an apparatus to predict the process of mixing in it [1, 8].

A number of scientific works [1, 6, 8, 13, 15] are devoted to the problems of the modeling of mixing processes. In our work, we have detailed the questions of the creation of a MU mathematical model, which would allow us to match the time-and-frequency characteristics of CCMs and dosers incorporated into a MU in the interactive operational mode of a computer. As a result, this provides the possibility of decreasing the amplitude of fluctuations in the output material flow of a mixer and improving the quality of a ready mixture.

**OBJECTS AND METHODS OF STUDY**

In the first case, the object of the study aimed at implementing the method of the sequential dilution of a mixture is a mixing unit that incorporates a block of two spiral and one batch dosers ( $D, i=1, N$ ) and two serially arranged CCMs. Spiral doser  $D_1$  and batch doser  $D_2$  deliver initial mixture components through summing element  $SE_1$  into  $CCM_1$ . This results in the mixing of components at a ratio of 1 : 500. The obtained mixture enters  $SE_2$ , into which the major component (incorporated into the mixture in a great amount) is simultaneously fed with spiral doser  $D_3$ , and then into  $CCM_2$ , where the components are finally mixed at a ratio of 1 : 20. As a result, the mixture with a ratio of mixed components of 1 : 1000 is obtained at the output of  $CCM_2$ .

The general structural functional scheme of the studied mixing unit operating by the method of the sequential dilution of a mixture is shown in Fig. 1. The dosers form the signals of the mass flow rates of materials that have masses  $Q_{d1}(t)$  and  $Q_{d2}(t)$  and concentrations  $X_{d1}(t)$  and  $X_{d2}(t)$  and are fed into  $SE_1$ , thereupon the summary flow with parameters  $X_{dc1}(t)$  and  $Q_{dc1}(t)$  enters  $CCM_1$ . The mixture that leaves the first mixer and has a weight  $Q_{M1}(t)$  and a concentration  $X_{M1}(t)$  and the material flow with parameters  $X_{d3}(t)$  and  $Q_{d3}(t)$  from spiral doser  $D_3$  are fed into  $SE_2$ . As a result, the material mass  $Q_{M1}(t)+Q_{d3}(t)$  with a concentration  $X_{M1}(t)+X_{d3}(t)$  enters  $CCM_2$ , and a mixture with parameters  $Q_{M2}(t)$  and  $X_{M2}(t)$  leaves it.

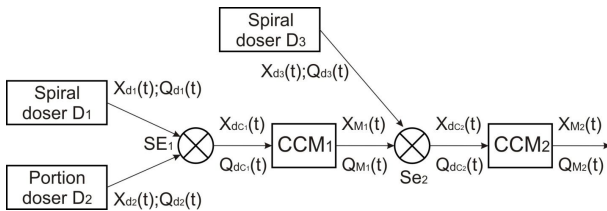


**Fig. 1. Structural functional scheme of the studied mixing unit.**

To perform the monitoring and control of the principal parameters of the continuous process of mixing, let us use the structural functional scheme implying the estimation of the impulse responses of dosers and the transfer functions of mixers that are incorporated into the MU [6, 9, 10]. The transfer function of a mixer is the ratio of the output signal  $y(S)$  to the input signal  $x(S)$ , both are Laplace transformed, at zero initial conditions. The transfer function is governed only by CCM internal properties, represents a dimensionless function of complex variables, and is denoted as  $W(S)=y(S)/x(S)$ .

From Fig. 1 it can be seen that the two-stage MU consists of the two blocks of dosers  $W_{DB1}(S)$  and  $W_{DB2}(S)$  that have certain impulse responses, form signals of different kinds, and operate in parallel for  $SE_1$  and  $SE_2$ . The principal elements of the scheme are the CCMs of new design developed by us with a horizontal rotor in the form of three and one hollow truncated cones ( $W_{CM1}(S)$  and  $W_{CM2}(S)$ ) [11, 12].

The MU output signal for the given scheme in the operator form ( $W_{MU}(S)$ ) is determined by the formula

$$W_{MU}(S) = [W_{DB1}(S) \times W_{CM1}(S) + W_{DB2}(S)] \times W_{CM2}(S), \quad (1)$$

where  $W_{DB1,2}(S)$  are the impulse responses of the block of dosers,  $W_{CM1,2}(S)$  is the CCM transfer function, and  $S$  is an independent complex variable that stands for differentiation with respect to time.

Here, the first block of dosers consists of a spiral doser and a batch doser. When the spiral doser forms a signal, the feed of a component  $X_{d1}(t)$  fluctuates by a time-dependent sinusoidal law with an average value  $X_{d01}$  and an amplitude  $X_{dm1}$ :

$$X_{d1}(t) = X_{d01} + X_{dm1} \times \sin(\omega_{d1}t), \quad (2)$$

Performing the Laplace transform of the given signal from the time-dependent form to the operator form, we obtain the following expression:

$$W_1(S) = \frac{X_{d01}}{S} + \frac{X_{dm1} \times \omega_{d1}}{S^2 + \omega_{d1}^2}, \quad (3)$$

where  $X_{d01}$  is the constant flow rate of a component dosed with a spiral doser and  $X_{dm1}$  and  $\omega_{d1}$  is the amplitude and frequency of fluctuations.

For the formation of a square-wave signal from the batch doser  $X_{d2}(t)$ , let us use the Fourier tenth-order expansion [6], which is represented by the following function in the temporal region:

$$X_{d2}(t) = \frac{A_{02}}{2} + \sum_{k=1}^{10} \left( A_{k2} \cdot \cos \frac{2k\pi}{T_{d2}} t + B_{k2} \cdot \sin \frac{2k\pi}{T_{d2}} t \right), \quad (4)$$

The Laplace transform of this signal gives the following expression:

$$W_2(S) = \frac{A_{02}}{2S} + \sum_{k=1}^{10} \left( \frac{A_{k2} \times S}{S^2 + \omega_{d2}^2} + \frac{B_{k2} \times \omega_{d2}}{S^2 + \omega_{d2}^2} \right), \quad (5)$$

where  $\omega_{k2}=2\pi k/T_{d2}$  is the angular fluctuation frequency corresponding to the  $k^{\text{th}}$  harmonic of the Fourier expansion of a square-wave signal from the batch doser,  $T_{d2}$  is the period of its fluctuations, and  $A_{02}$ ,  $A_{k2}$ , and  $B_{k2}$  are coefficients in the Fourier expansion of the signal.

$$\begin{cases} A_{02} = \frac{2}{T_{d2}} \int_0^{T_{d2}} X(t) dt \\ A_{k2} = \frac{2}{T_{d2}} \int_0^{T_{d2}} X(t) \times \cos \left( \frac{2k\pi}{T_{d2}} t \right) dt, \\ B_{k2} = \frac{2}{T_{d2}} \int_0^{T_{d2}} X(t) \times \sin \left( \frac{2k\pi}{T_{d2}} t \right) dt \end{cases} \quad (6)$$

Then, taking into account Eqs. (3) and (5), the summary signal  $W_{DB1}(S)$  in the operator form will be



real dosing impulses. From the block structural scheme it can be seen that it has two inputs and one output.

Let us transform the obtained transfer functions (Eqs. (7), (9), and (12)) into the corresponding differential equations. By way of example, let us consider the first summand of Eq. (7)  $\frac{X_{d01}}{S}u(t)$ , which is the image of the function  $y_1(t)$ , i.e.,  $\frac{X_{d01}}{S}u(t) = Y_1 \rightarrow y_1$ . Multiplying both sides of the equation by  $S$  with consideration for  $S \times Y_1 \rightarrow \dot{y}_1$ , we obtain the differential equation  $\dot{y}_1 = X_{d01} \times u(t)$ . Transforming the other elements (summands) in a similar way, we obtain the following system of differential equations:

$$\left\{ \begin{aligned} \frac{dy_1(t)}{dt} &= X_{d01} \times u(t) \\ \frac{d^2 y_2(t)}{dt^2} + \omega_{d1}^2 \times y_2(t) &= X_{dm1} \times \omega_{d1} \times u(t) \\ \frac{dy_3(t)}{dt} &= \frac{A_0}{2} \times u(t) \\ \frac{d^2 y_4(t)}{dt^2} + \omega_{d2}^2 \times y_4(t) &= A_1 \times u(t) \\ \frac{d^2 y_5(t)}{dt^2} + \omega_{d2}^2 \times y_5(t) &= B_1 \times \omega_{d2} \times u(t) \\ \frac{d^2 y_6(t)}{dt^2} + 4\omega_{d2}^2 \times y_6(t) &= A_2 \times u(t) \\ \frac{d^2 y_7(t)}{dt^2} + 4\omega_{d2}^2 \times y_7(t) &= 2B_2 \times \omega_{d2} \times u(t) \\ \frac{d^2 y_8(t)}{dt^2} + 9\omega_{d2}^2 \times y_8(t) &= A_3 \times u(t) \\ \frac{d^2 y_9(t)}{dt^2} + 9\omega_{d2}^2 \times y_9(t) &= 3B_3 \times \omega_{d2} \times u(t) \\ \dots\dots\dots \\ \frac{d^2 y_{22}(t)}{dt^2} + 100\omega_{d2}^2 \times y_{22}(t) &= A_{10} \times u(t) \\ \frac{d^2 y_{23}(t)}{dt^2} + 100\omega_{d2}^2 \times y_{23}(t) &= 10B_{10} \times \omega_{d2} \times u(t) \\ T_2 \frac{d^2 y_{24}(t)}{dt^2} + T_1 \frac{dy_{24}(t)}{dt} + y_{24}(t) &= Km \sum_{i=1}^{23} y_i \\ \frac{d^2 y_{25}(t)}{dt^2} + \omega_{d3}^2 \times y_{25}(t) &= X_{dm3} \times \omega_{d3} \times u(t) \\ \frac{dy_{26}(t)}{dt} &= X_{d03} \times u(t) \\ T_1' \frac{dy(t)}{dt} + y(t) &= Km(y_{24}(t) + y_{25}(t) + y_{26}(t)) \end{aligned} \right. , \quad (13)$$

where  $y_1(t), y_2(t), y_3(t), y_4(t) \dots y_{25}(t)$  are the internal signals that characterize the operation of corresponding transfer functions in the elements of the block structural scheme. The sum of  $y_1(t)$  and  $y_2(t)$  is the signal formed by the spiral doser, and the sum of  $y_3(t), y_4(t) \dots y_{23}(t)$  is the signal formed by the batch dosers in the first block. The signals  $y_{25}(t)$  and  $y_{26}(t)$  are formed by the spiral

doser of the second block,  $y_{24}(t)$  corresponds to the output signal of the first-stage CCM, and  $y(t)$  corresponds to the output signal of the second-stage CCM or the MU as a whole.

To solve system (14), let us reduce the order of the differential equations via the substitution of variables.

$$\begin{pmatrix} y_1(t) \\ y_2(t) \\ \dot{y}_2(t) \\ y_3(t) \\ \dots\dots\dots \\ y_k(t) \\ \dot{y}_k(t) \\ \dots\dots\dots \\ y_{26}(t) \\ y(t) \end{pmatrix} = \begin{pmatrix} x_1(t) \\ x_2(t) \\ x_3(t) \\ x_4(t) \\ \dots\dots\dots \\ x_{2k-3}(t) \\ x_{2k-2}(t) \\ \dots\dots\dots \\ x_{49}(t) \\ x_{50}(t) \end{pmatrix}, \quad (k = \overline{4,25}), \quad (14)$$

Such a transformation allows us to write the system of the differential equations describing the behavior of the MU with a batch doser signal that has  $n$  Fourier expansion harmonics in the Cauchy normal form.

$$\left\{ \begin{aligned} \dot{x}_1(t) &= X_{d01} \times u(t) \\ \dot{x}_2(t) &= x_3(t) \\ \dot{x}_3(t) &= -\omega_{d1}^2 \times x_2(t) + X_{dm1} \times \omega_{d1} \times u(t) \\ \dot{x}_4(t) &= \frac{A_0}{2} \times u(t) \\ \dot{x}_{4k+1}(t) &= x_{4k+2}(t) \quad (k = \overline{1,n}) \\ \dot{x}_{4k+2}(t) &= -k^2 \times \omega_{d2}^2 \times x_{4k+1}(t) + A_k \times u(t) \\ \dot{x}_{4k+3}(t) &= x_{4k+4}(t) \\ \dot{x}_{4k+4}(t) &= -k^2 \times \omega_{d2}^2 \times x_{4k+3}(t) + kB_k \times \omega_{d2} \times u(t) \\ \dot{x}_{4n+5}(t) &= x_{4n+6}(t) \\ \dot{x}_{4n+6}(t) &= \frac{Km}{T_2} (x_1(t) + x_2(t) + x_4(t) + \sum_{k=1}^{2n} x_{2k+3}(t)) - \\ &\quad - \frac{1}{T_2} \times x_{4n+5}(t) - \frac{T_1}{T_2} \times x_{4n+6}(t) \\ \dot{x}_{4n+7}(t) &= x_{4n+8}(t) \\ \dot{x}_{4n+8}(t) &= -\omega_{d3}^2 \times x_{4n+7}(t) + X_{dm3} \times \omega_{d3} \times u(t) \\ \dot{x}_{4n+9}(t) &= X_{dm3} \times u(t) \\ \dot{x}_{4n+10}(t) &= \frac{Km}{T_1'} (x_{4n+5}(t) + x_{4n+7}(t) + x_{4n+9}(t)) - \frac{1}{T_1'} \times x_{4n+10}(t) \end{aligned} \right. , \quad (15)$$

It should be noted that the output signal  $y(t)$  of the second CCM is related with the state variable  $x_{4n+10}(t)$  according to Eq. (15) via the relationship  $y(t) = x_{4n+10}(t)$ , which is the output equation for the considered MU.

Obtained model (16) that contains information on the formation of flow signals in the blocks of dosers also allows us to trace their fluctuations in parallel (during a single calculation procedure) with the output

signal that has passed the first CCM and is received at the output of the second mixer.

Let us model a two-stage MU consisting of three spiral dosers and two CCMs in a similar manner. Its structural functional scheme is shown in Fig. 3.

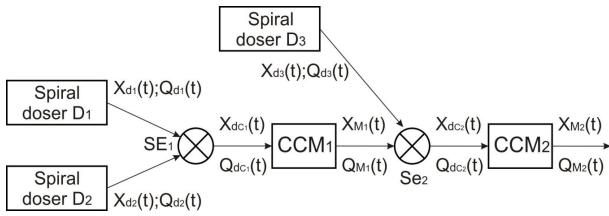


Fig. 3. Structural functional scheme of the mixing unit.

The output signal of the MU, where the first block incorporates two spiral dosers, in the operator form ( $W_{MU}(S)$ ) is represented by Eq. (1), and its impulse response is determined as

$$W_{DB1}(S) = \frac{X_{d01}}{S} + \frac{X_{dm1} \times \omega_{d1}}{S^2 + \omega_{d1}^2} + \frac{X_{d02}}{S} + \frac{X_{dm2} + \omega_{d2}}{S^2 + \omega_{d2}^2}, \quad (16)$$

The second block incorporates a spiral doser, whose impulse response is represented by Eq. (9). The transfer functions of the mixers are expressed by Eqs. (10) and (11).

Substituting the impulse responses of all the MU blocks and apparatuses (Eqs. (16), (9), (10), and (11)) into Eq. (1), we obtain the following model for the process of the mixing of bulk materials:

$$W_{MU}(S) = \left[ \left( \frac{X_{d01}}{S} + \frac{X_{dm1} \times \omega_{d1}}{S^2 + \omega_{d1}^2} + \frac{X_{d02}}{S} + \frac{X_{dm2} + \omega_{d2}}{S^2 + \omega_{d2}^2} \right) \times \frac{K \times e^{-\tau S}}{T_2 \times S^2 + T_1 \times S + 1} + \frac{X_{d03}}{S} + \frac{X_{dm3} \times \omega_{d3}}{S^2 + \omega_{d3}^2} \right] \times \frac{K \times e^{-\tau S}}{T_1 \times S + 1}, \quad (17)$$

Let us consider a procedure in the space of MU model states and, to accomplish this, transform the general structural functional scheme of the studied MU (Fig. 3) into the scalarized block structural scheme (Fig. 4).

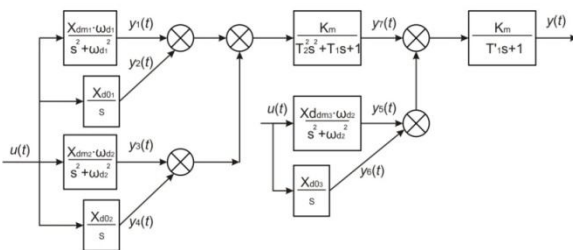


Fig. 4. Block structural scheme of the mixing unit.

Applying the above considered expressions, we write the following system of differential equations:

$$\begin{cases} \frac{d^2 y_1(t)}{dt^2} + \omega_{d1}^2 \times y_1(t) = X_{dm1} \times \omega_{d1} \times u(t) \\ \frac{dy_2(t)}{dt} = X_{d01} \times u(t) \\ \frac{d^2 y_3(t)}{dt^2} + \omega_{d2}^2 \times y_3(t) = X_{dm2} \times \omega_{d2} \times u(t) \\ \frac{dy_4(t)}{dt} = X_{d02} \times u(t) \\ \frac{d^2 y_5(t)}{dt^2} + \omega_{d3}^2 \times y_5(t) = X_{dm3} \times \omega_{d3} \times u(t) \\ \frac{dy_6(t)}{dt} = X_{d03} \times u(t) \\ T_2 \frac{d^2 y_7(t)}{dt^2} + T_1 \frac{dy_7(t)}{dt} + y_7(t) = K_m (y_1(t) + y_2(t) + y_3(t) + y_4(t)) \\ T_1 \frac{dy_8(t)}{dt} + y_8(t) = K_m (y_5(t) + y_6(t) + y_7(t)) \end{cases}, \quad (18)$$

To solve it, let us reduce the order of the differential equations.

$$\begin{pmatrix} y_1(t) \\ \dot{y}_1(t) \\ y_2(t) \\ y_3(t) \\ \dot{y}_3(t) \\ y_4(t) \\ y_5(t) \\ \dot{y}_5(t) \\ y_6(t) \\ y_7(t) \\ \dot{y}_7(t) \\ y_8(t) \\ y(t) \end{pmatrix} = \begin{pmatrix} x_1(t) \\ x_2(t) \\ x_3(t) \\ x_4(t) \\ x_5(t) \\ x_6(t) \\ x_7(t) \\ x_8(t) \\ x_9(t) \\ x_{10}(t) \\ x_{11}(t) \\ x_{12}(t) \end{pmatrix}, \quad (19)$$

Using Eqs. (18) and (19) as a basis, we obtain the resulting equation system (in the Cauchy normal form) describing the behavior of the mixing unit:

$$\begin{cases}
 \dot{x}_1(t) = x_2(t) \\
 \dot{x}_2(t) = -\omega_{d2}^2 \times x_1(t) + X_{dm1} \times \omega_{d1} \times u(t) \\
 \dot{x}_3(t) = X_{a01} \times u(t) \\
 \dot{x}_4(t) = x_5(t) \\
 \dot{x}_5(t) = -\omega_{d2}^2 \times x_4(t) + X_{dm2} \times \omega_{d2} \times u(t) \\
 \dot{x}_6(t) = X_{a02} \times u(t) \\
 \dot{x}_7(t) = x_8(t) \\
 \dot{x}_8(t) = -\omega_{d3}^2 \times x_7(t) + X_{dm3} \times \omega_{d3} \times u(t) \\
 \dot{x}_9(t) = X_{a03} \times u(t) \\
 \dot{x}_{10}(t) = x_{11}(t) \\
 \dot{x}_{11}(t) = \frac{K_m}{T_2} (x_1(t) + x_3(t) + x_4(t) + x_6(t)) - \\
 \quad - \frac{1}{T_2} \times x_{10}(t) - \frac{T_1}{T_2} \times x_{11}(t) \\
 \dot{x}_{12}(t) = \frac{K_m}{T_1'} (x_7(t) + x_9(t) + x_{10}(t)) - \frac{1}{T_1'} \times x_{12}(t)
 \end{cases}, (20)$$

According to Eq. (19), the output equation for the considered MUs is

$$y(t) = x_{12}(t), \quad (21)$$

The obtained models can be implemented via different mathematical software that provides the possibility of calculating the MU time-and-frequency characteristics using the known values of doser impulse responses and mixer transfer functions.

**RESULTS AND DISCUSSION**

The frequency method of determining the smoothening degree requires the knowledge of the frequency transfer function of a mixer that operates in a certain regime (rotor speed, internal and external recycle ratios, taper angle, etc.). The given studies were performed on the white flour–potassium iodide mixture.

To determine the smoothability of the two centrifugal MUs (the first of them is schematized in Fig. 1, and the scheme of the second MU is shown in Fig. 2), the transfer functions of the mixers incorporated in them were represented as  $W(j\omega) = j \times \text{Im}(\omega) + \text{Re}(\omega)$ . After  $\text{Re}(\omega)$  and  $\text{Im}(\omega)$  were determined, we plotted the amplitude frequency characteristic  $A(\omega) = \sqrt{(\text{Im}^2(\omega) + \text{Re}^2(\omega))}$ .

The studied MUs contain two CCMs each and identical spiral dosers, whose frequencies will be used to estimate the smoothability. For this reason, the obtained amplitude frequency characteristics will be identical for both mixing units.

Hence, the amplitude frequency characteristics of the first-stage CCMs of the studied MUs are plotted in Fig. 5.

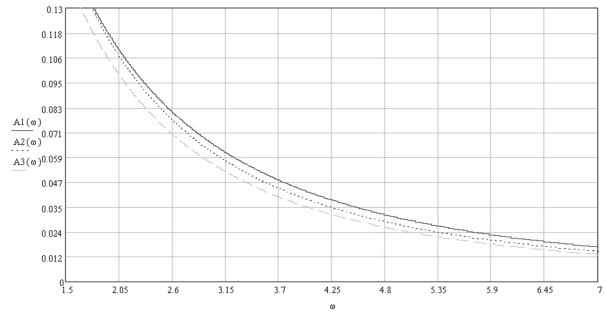


**Fig. 5. Amplitude frequency characteristics A1, A2, and A3 of CCM rotor speeds for the three operational regimes [12] at 10, 12.5, and 15 s<sup>-1</sup>, respectively.**

From Fig. 5 it can be seen that the MU operating in the third regime has the best smoothing characteristics. The CCM smoothability was estimated from the plots for the third operational regime at a specified operational frequency of dosers. For example, if a dosing signal with a frequency  $\omega = 4.02 \text{ s}^{-1}$  is sent to the input of a mixer (first doser signal), the length of the transfer function vector is  $R(\omega) = A(\omega) = 0.032$ . The smoothability of the first-stage centrifugal mixer was then determined as

$$S(4.02) = \frac{1}{R(4.02)} = \frac{1}{0.032} = 31.25, \quad (22)$$

Hence, the centrifugal mixer smoothenes feed flow fluctuations at the given frequency of input signals by 31.25 times.

Let us further consider the amplitude frequency characteristic for the second-stage CCM [11] of the studied MUs (Fig. 6).

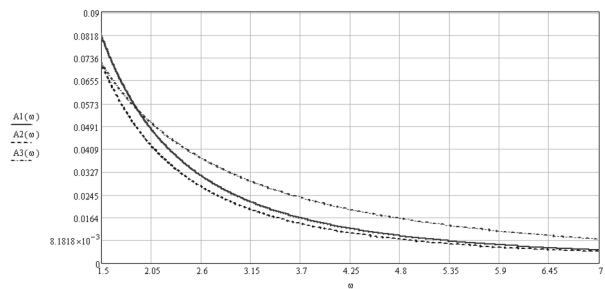


**Fig. 6. Amplitude frequency characteristics A1, A2, and A3 of CCM rotor speeds for the three operational regimes at 10, 12.5, and 15 s<sup>-1</sup>, respectively.**

If a dosing signal with a frequency  $\omega = 4.02 \text{ s}^{-1}$  (third doser signal) is sent to the input of the mixer (at  $n = 15 \text{ s}^{-1}$ ), the length of the frequency transfer function vector is  $R(\omega) = A(\omega) = 0.0123$ . The smoothability of the first-stage centrifugal mixer is further determined as

$$S(4.02) = \frac{1}{R(4.02)} = \frac{1}{0.0123} = 81.3, \quad (23)$$

Hence, the centrifugal mixer smoothenes feed flow

fluctuations at the given frequency of input signals by 81.3 times.

The data for all the MU operational regimes are given in Table 1.

**Table 1. Smoothability of the mixing units**

	CCM operational regimes (rotor speed, s <sup>-1</sup> )	Input signal frequency, s <sup>-1</sup>	
		2.093	4.02
White flour potassium iodide mixture			
First-stage CCM [1]	10	9.17	24.39
	12.5	9.43	28.57
	15	10.00	31.25
Second-stage CCM [4]	10	20.36	45.87
	12.5	24.44	91.46
	15	19.23	81.3
MU	10	29.53	70.26
	12.5	33.87	120.03
	15	39.53	112.55

Hence, it follows from the results of frequency analysis that the smoothability ( ) grows with an increase in the operational speeds of CCM rotors and the input signals formed by the dosers. Its considerable growth occurs upon the switch from the first CCM operational regime to the second regime at both stages. The highest value of ( ) for the studied MUs is observed at a CCM rotor speed of 12.5 s<sup>-1</sup>.

To determine the degree of the smoothening of real dosing station signals, we also performed the time analysis of the MUs.

Let us first perform the analysis of the first MU (Fig. 1) at a CCM rotor speed of 10 s<sup>-1</sup>. Let us determine the real signal of the MU first-stage doser block from Eq. (2) using, for example, the *MathCAD* software for the case when the major component (white flour) is dosed with a spiral doser and the key component (potassium iodide) is dosed with a batch doser. The concentration of potassium iodide in the flour was found potentiometrically on an Elis-131-1 ion selective electrode, with which the equilibrium concentration of iodine ions in a solution was determined. The measurements of pI were performed on an ANION-4100 ion conductivity meter. The iodide selective electrode was preliminary calibrated against standard potassium iodide solutions with a mass concentration of 2. 1.5, 1, 0.5, and 0.1 g/dm<sup>3</sup> [3]. The obtained signal is shown in Fig. 7.

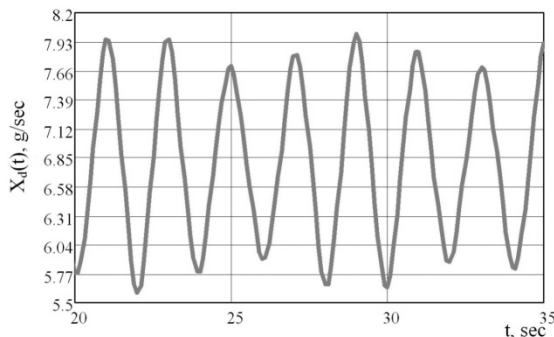


**Fig. 7. Signal of the first block of dosers (spiral and batch).**

The amplitude of the input signal of the first block of dosers is

$$X_{dm}^{IN} = \frac{X_{d0}^{max} - X_{d0}^{min}}{2} = \frac{8.036 - 5.564}{2} = 1.236, \text{ g/s. (24)}$$

The obtained signal was further sent to the input of the MU first-stage CCM [12]. The response of the system to the input signal is shown in Fig. 8.

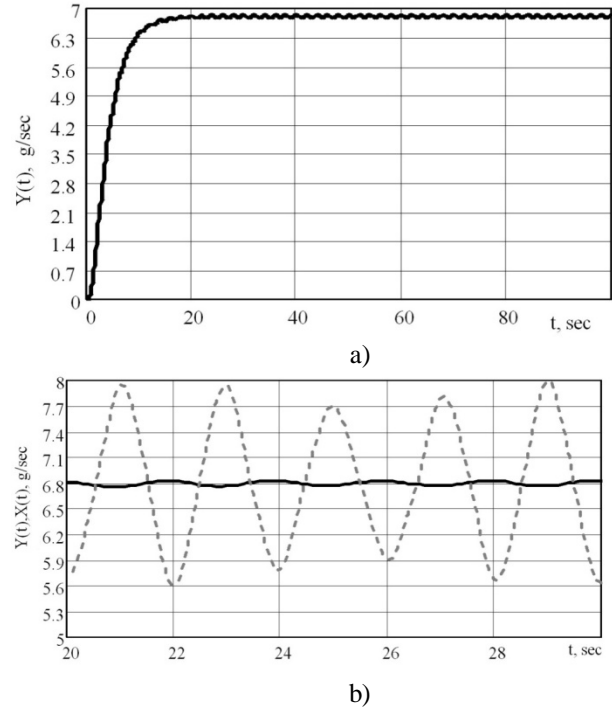


**Fig. 8. Response of the system to the input signal of the first block of dosers: (a) output signal of the first-stage centrifugal mixer, (b) ratio of the amplitudes of the input (---) and (—) output signals.**

The analysis of the obtained plots allows us to determine the real degree of the smoothening of feed flow fluctuations for the first block of dosers and also the numerical values of the real transfer functions of the first-stage CCMs  $W_{CMI}(S)$ .

By way of example, let us calculate  $S(\omega)$  of a CCM. To accomplish this, let us calculate the amplitude of the mixer's output signal by the formula

$$X_{dm}^{OUT} = \frac{X_{d0}^{max} - X_{d0}^{min}}{2} = \frac{6.832 - 6.766}{2} = 0.033, \text{ g/s. (25)}$$

Then we find

$$R(\omega) = \frac{X_{dm}}{X_{d0}} = \frac{0.033}{6.799} = 0.00482, \quad (26)$$

Thereupon we calculate the mixer's smoothability as

$$S(\omega) = \frac{1}{R(\omega)} = \frac{1}{0.00482} = 207.22, \quad (27)$$

The CCM transfer function can be calculated from the ratio of the amplitudes of the input and output signals, and its numerical value is then equal to

$$W_{CM1}(S) = \frac{X_{dm}^{OUT}}{X_{dm}^{IN}} = \frac{0.033}{1.236} = 0.027, \quad (28)$$

The smoothability of the mixer at rotor speeds of 12.5 and 15 s<sup>-1</sup> was determined in a similar way. The obtained results were compiled in Table 2.

**Table 2. Smoothability and transfer function of the first-stage mixer**

$n, s^{-1}$	$X_{dm}, g/s$	$X_{dm}^{OUT}, g/s$	(*)	(**)
10	1.236	0.033	207.22	0.027
12.5	1.236	0.031	222.9	0.025
15	1.236	0.025	272.9	0.02

\* is the fluctuation frequency created by a doser, s<sup>-1</sup>.

\*\* S is an independent complex variable that stands for differentiation with respect to time.

The results of the performed analysis indicate that the CCM [12] smoothens well input material flow fluctuations produced by the first block of volumetric dosers. The best result was obtained at a rotor speed of 15 s<sup>-1</sup>.

The signal from the second block of dosers was then superimposed to the output signal of the first-stage CCM, thus leading to an increase in its amplitude and the numerical value of its impulse response (signals from the first-stage CCM and the second-stage block of dosers). The graphical interpretation of the given signal is shown in Fig. 9.

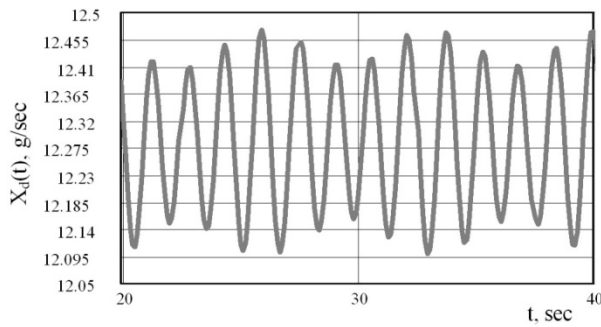


**Fig. 9. Summary signal from the first CCM and the second block of dosers.**

The amplitude of this signal is equal to

$$X_{dm}^{IN} = \frac{X_{d0}^{max} - X_{d0}^{min}}{2} = \frac{12.474 - 12.098}{2} = 0.188, \text{ g/s.} \quad (29)$$

To determine the impulse response of the first-stage CCM and the second-stage block of dosers, the amplitude calculated by Eq. (30) should be divided by  $X_{dm}^{IN}$  obtained by Eq. (26):

$$W_{CM1+BD2}(S) = \frac{X_{dm}^{OUT}}{X_{dm}^{IN}} = \frac{0.1883}{0.033} = 5.371, \quad (30)$$

The obtained signal was further sent to the input of the MU second-stage CCM [11]. The response of the system to the input signal is shown in Fig. 10.

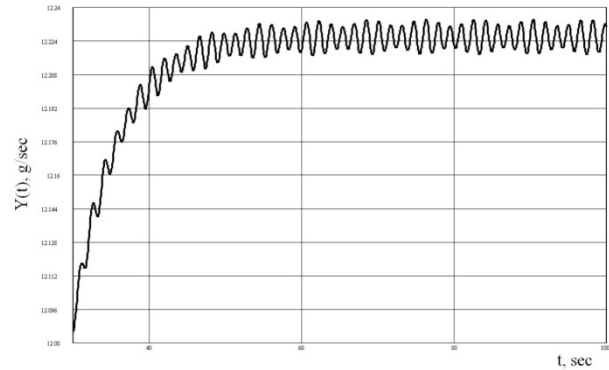


**Fig. 10. Response of the system to the input signal of the second-stage block of dosers and the first CCM.**

The ratios of the amplitudes of the input and output signals for the second CCM [11] are plotted in Fig. 11.

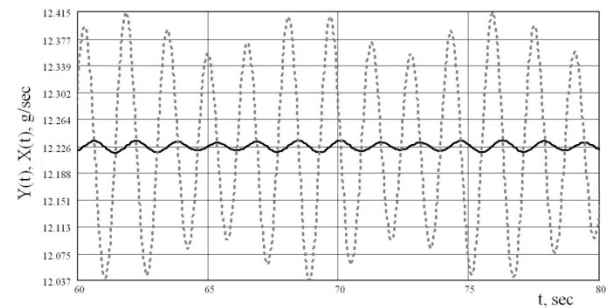


**Fig. 11. Magnified system response fragment for the steady-state operational regime. Ratio of the amplitudes of the input (---) and output (—) signals.**

Since the second-stage CCM is the end element in the functional structural scheme (Fig. 1), its output signal  $y(t)$  may be considered as the output impulse of the entire studied MU, and the transfer function  $W_{CM2}(S)$  becomes  $W_{MU}(S)$ .

For further analysis, let us calculate  $S(\omega)$  and  $W_{CM2}(S)$  of the CCM at  $n = 10 \text{ s}^{-1}$ . To accomplish this, let us calculate the amplitude of the mixer's output signal by the formula

$$X_{dm}^{OUT} = \frac{X_{d0}^{max} - X_{d0}^{min}}{2} = \frac{12.294 - 12.144}{2} = 0.075, \text{ g/s.} \quad (31)$$

Further, we find

$$R(\omega) = \frac{X_{dm}^{OUT}}{X_{d0}} = \frac{0.075}{12.219} = 0.00614, \quad (32)$$

Then we determine the smoothability of the mixer as

$$S(\omega) = \frac{1}{R(\omega)} = \frac{1}{0.00614} = 162.867, \quad (33)$$

The transfer function of the second-stage CCM (or the MU transfer function) will be

$$W_{NI\ 2}(S) = \frac{X_{dm}^{OUT}}{X_{dm}^{IN}} = \frac{0.075}{0.188} = 0.399, \quad (34)$$

The smoothability of the second-stage mixer and its transfer function at rotor speeds of 12.5 and 15 s<sup>-1</sup> was determined in a similar way. The obtained results were compiled in Table 3.

The results of the performed analysis indicate that the second-stage CCM [11] slightly worse smoothens input material flow fluctuations in comparison with the first-stage CCM [12]. This is explained by that the rotor of the second mixer consists of a single cone, so mixed particles reside in the working zone of the mixer for a shorter time.

Let us further perform the analysis of the second MU, whose regime parameters are the same as for the first MU. The real signal of the first-stage block of MU spiral dosers was determined by Eq. (15) for the white flour potassium iodide feed. The obtained signal is plotted in Fig. 12.

**Table 3. Smoothability and transfer function of the second-stage mixer**

$n, s^{-1}$	First mixer and second block of dosers		Second mixer or mixing unit		
	$X, g/s$	( )	$X, g/s$	( *)	( **)
10	0.188	5.37	0.075	162.86	0.399
12.5	0.186	6.103	0.11	111.2	0.59
15	0.182	3.15	0.109	111.6	0.595

\* is the fluctuation frequency created by a doser, s<sup>-1</sup>.

\*\* S is an independent complex variable that stands for differentiation with respect to time.

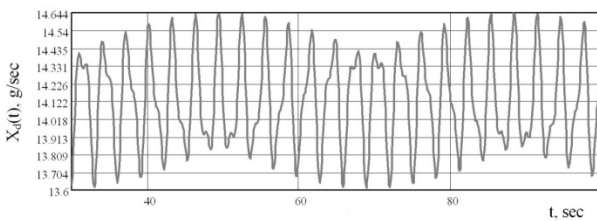


**Fig. 12. Signal of the first block of dosers (both are spiral).**

The amplitude of the given signal is  $X_{dm}^{IN} = 0.516$  g/s.

Sending the given signal to the input of the MU first-stage CCM [12], we obtain the system's response shown in Fig. 13.

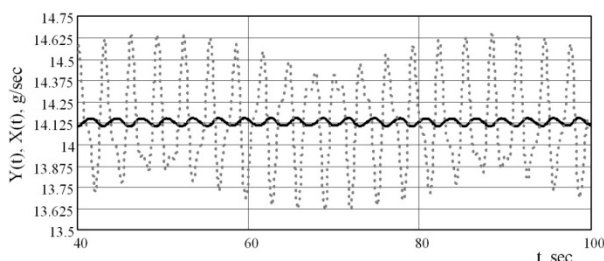


**Fig. 13. Magnified system response fragment. Ratio of the amplitudes of the input (---) and output (—) signals.**

The output signal amplitude is  $X_{dm}^{OUT} = 0.025$  g/s.

The ratio of the amplitude to the average mass flow rate is  $R(\omega) = 0.0018$ .

Then the smoothability of the first-stage CCM is

$$S(\omega) = \frac{1}{R(\omega)} = \frac{1}{0.0018} = 554.67, \quad (35)$$

and its transfer function is

$$W_{CM1}(S) = \frac{X_{dm}^{OUT}}{X_{dm}^{IN}} = \frac{0.025}{0.516} = 0.049, \quad (36)$$

The parameters of the implementation of the mathematical model of the MU first stage for the operation of the CCM at rotor speeds of 12.5 and 15 s<sup>-1</sup> are given in Table 4.

**Table 4. Smoothability and transfer function of the first-stage mixer**

$n, s^{-1}$	$X, g/s$	$X, g/s$	( *)	( **)
10	0.516	0.025	554.67	0.049
12.5	0.516	0.025	591.13	0.046
15	0.516	0.02	716.46	0.038

\* is the fluctuation frequency created by a doser, s<sup>-1</sup>.

\*\* S is an independent complex variable that stands for differentiation with respect to time.

From Table 4 it can be seen that the CCM [12] has the highest smoothability at a rotor speed of 15 s<sup>-1</sup>.

Further, the output signals of the first-stage CCM and the second block of dosers superimpose over each other. The graphical interpretation of the summary signal is shown in Fig. 14.

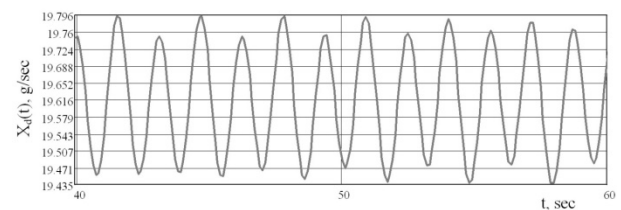


**Fig. 14. Summary signal from the first CCM and the second block of dosers.**

The amplitude of the given signal and the CCM transfer function are  $X_{dm}^{IN} = 0.181$  g/s and  $W_{CM1+BD2}(S) = 7.1$ , respectively.

The obtained signal was sent to the input of the MU second-stage CCM [11]. The response of the system to the input signal is shown in Fig. 15.

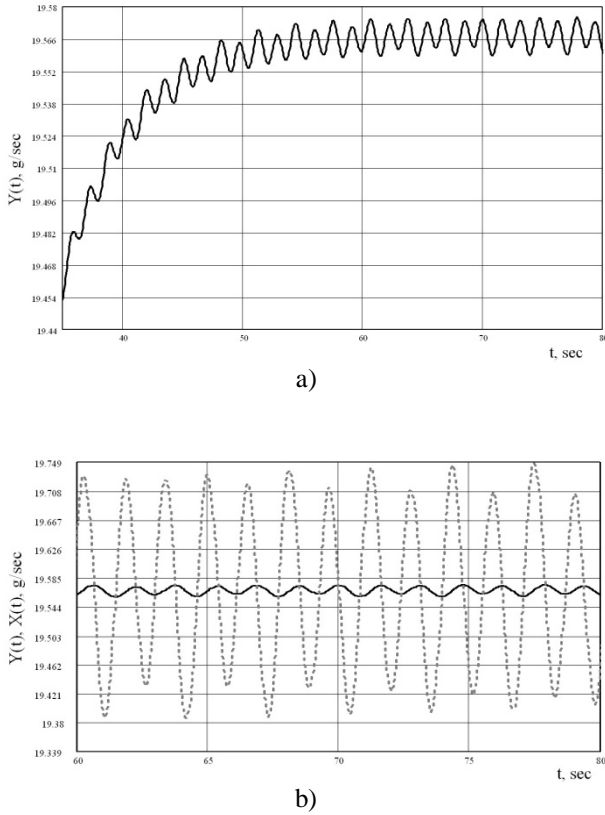


**Fig. 15. Response of the system to the input signal of the first block of dosers and the continuous centrifugal mixer: (a) output signal of the second-stage CCM, (b) magnified fragment of the ratio of the amplitudes of the input (---) and output (—) signals.**

The amplitude of the output signal of the second-stage mixer is

$$X_{dm}^{OUT} = \frac{X_{d0}^{max} - X_{d0}^{min}}{2} = \frac{19.624 - 19.606}{2} = 0.00889, \text{ g/s.} \quad (37)$$

$$R(\omega) = \frac{X_{dm}}{X_{d0}} = \frac{0.00889}{19.615} = 0.00045, \quad (38)$$

The smoothability of the second-stage CCM is

$$S(\omega) = \frac{1}{R(\omega)} = \frac{1}{0.00045} = 2204, \quad (39)$$

The transfer function of the second-stage CCM (or the MU) is

$$W_{CM2}(S) = \frac{X_{dm}^{OUT}}{X_{dm}^{IN}} = \frac{0.00889}{0.181} = 0.049, \quad (40)$$

The results obtained at rotor speeds of 12.5 and 15 s<sup>-1</sup> are given in Table 5.

**Table 5. Smoothability and transfer function of the second-stage mixer**

$n, \text{ s}^{-01}$	First mixer and second block of dosers		Second mixer or mixing unit		
	$X, \text{ g/s}$	( )	$X, \text{ g/s}$	( *)	( **) ( )
10	0.181	7.1	0.00889	2204	0.049
12.5	0.18	7.51	0.0088	2228	0.049
15	0.176	8.94	0.025	797.95	0.139

\* is the fluctuation frequency created by a doser, s<sup>-1</sup>.

\*\* S is an independent complex variable that stands for differentiation with respect to time.

The results of the performed analysis indicate that the second-stage CCM [11] has the same numerical values of the transfer function as for the first-stage CCM [12]. The difference exists only between the values obtained at  $n = 15 \text{ s}^{-1}$ , thus confirming the fact that the mixture components reside in the working zone of a mixer for a minimum period of time. For this reason, the second-stage CCM has not enough time to smoothen input flow fluctuations to an adequate degree.

Let us further consider some parameters of the implementation of the mathematical model of the studied MUs on the sugar-millet, salt-semolina, and river sand-ferromagnetic powder mixtures from Table 6 and 7.

Hence, the operational frequency regimes of dosers and CCMs have been matched for the preparation of high-quality mixtures with a high ratio of mixed components on the basis of cybernetic approach with some ACT elements. Theoretical and experimental analyses have allowed us to determine the obtained result error, which does not exceed  $\pm 10.56 \%$ . Consequently, the represented models adequately describe the obtained experimental data.

The smoothabilities of mixers with respect to input material flow fluctuations have been determined using the frequency and time methods. Their numerical values lie within a range from 50 to 2230 times. The discrepancy between the results of time-and-frequency analyses in the case of obtaining the white flour-potassium iodide mixture at a CCM rotor speed of 12.5 s<sup>-1</sup> is 8.1%. Hence, the use of these methods of analysis is absolutely allowable.

The implementation of the mathematical models of mixing units that operate by the principle of the sequential dilution of a mixture shows that the best smoothability is attained for the mixing of components at first- and second-stage CCM rotor speeds of 15 and 10 s<sup>-1</sup>, respectively.

It has been established that it is necessary to prolong the time of the residence of mixed components in the working zone by sequentially passing them through a greater number of cones to increase the smoothability of mixers.

**Table 6. Smoothability and transfer function of the first mixing unit**

First CCM					First CCM and second block of dosers		Second CCM or mixing unit		
$n, s^{-1}$	$X, g/s$	$X, g/s$	(*)	(**)	$X, g/s$	( )	$X, g/s$	(*)	(**)
Sugar-millet mixture									
10	1.35	0.042	287.9	0.031	0.363	8.69	0.029	775.7	0.081
12.5	1.35	0.028	430	0.021	0.354	12.65	0.292	77.35	0.825
15	1.35	0.03	404.8	0.022	0.355	11.94	0.071	322	0.2
Salt-semolina mixture									
10	1.47	0.012	1478	0.0082	0.383	31.65	0.066	522.4	0.173
12.5	1.47	0.018	1012	0.012	0.386	21.83	0.037	942.7	0.095
15	1.47	0.012	1502	0.008	0.383	32.1	0.038	910.2	0.1
River sand-ferromagnetic powder mixture									
10	1.23	0.04	220.97	0.033	0.262	6.55	0.022	772.5	0.083
12.5	1.23	0.03	294.14	0.024	0.255	8.47	0.023	740.1	0.089
15	1.23	0.027	332.36	0.022	0.252	9.48	0.023	742	0.09

\*  $\omega$  is the fluctuation frequency created by a doser,  $s^{-1}$ .

\*\*  $S$  is an independent complex variable that stands for differentiation with respect to time.

**Table 7. Smoothability and transfer function of the second mixing unit**

First CCM					First CCM and second block of dosers		Second CCM or mixing unit		
$n, s^{-1}$	$X, g/s$	$X, g/s$	(*)	(**)	$X, g/s$	( )	$X, g/s$	(*)	(**)
Sugar-millet mixture									
10	0.65	0.031	514.1	0.048	0.353	11.21	0.028	965.3	0.079
12.5	0.65	0.031	761.2	0.033	0.348	16.35	0.017	1593	0.049
15	0.65	0.022	726	0.034	0.348	15.61	0.02	1357	0.057
Salt-semolina mixture									
10	0.93	0.006	3451	0.0069	0.381	58.75	0.079	496.9	0.207
12.5	0.93	0.006	1868	0.013	0.385	32.15	0.042	926.2	0.11
15	0.93	0.008	2734	0.0087	0.382	46.71	0.044	892	0.115
River sand-ferromagnetic powder mixture									
10	0.63	0.037	275.4	0.058	0.259	7.087	0.022	824.4	0.084
12.5	0.63	0.037	362.8	0.044	0.253	9.113	0.023	780.3	0.091
15	0.63	0.025	409.3	0.039	0.251	10.187	0.019	924.6	0.078

\*  $\omega$  is the fluctuation frequency created by a doser,  $s^{-1}$ .

\*\*  $S$  is an independent complex variable that stands for differentiation with respect to time.

The developed mathematical models have allowed us to compare the operational efficiency of two centrifugal MUs. The analysis of results shows that the

second MU that incorporates three spiral dosers has the highest smoothability.

## REFERENCES

1. Akhmadiev, F.G. and Aleksandrovskii, A.A., Modelirovanie i realizatsiya sposobov prigotovleniya smesei (Modeling and implementation of mixture preparation methods), *Zhurnal Vsesoyuznogo Khimicheskogo Obshchestva imeni D.I. Mendeleeva (Journal of All-Union Mendeleev Chemical Society)*, 1988, vol. 33, no. 4, p. 448.
2. Borodulin, D.M. and Ivanets, V.N., *Razvitie smesitel'nogo oborudovaniya tsentrobezhnogo tipa dlya polycheniya sukhikh i uvlazhnennykh kombinirovannykh produktov (Development of Centrifugal Mixing Equipment for the Preparation of Dry and Wetted Combined Food Products)*, Kemerovo: KemTIPP, 2012.
3. Gel'man, M.I. and Kirsanova, N.V., *Praktikum po fizicheskoi khimii. Uchebnoe posobie (Workshop on Physical Chemistry: Tutorials)*, St. Petersburg: Lan', 2004.
4. Ivanets, V.N., Smesiteli poroshkoobraznykh materialov dlya vitaminizatsii pishchevykh i kormovykh produktov (Mixers of powder-like materials for the vitaminization of food and fodder products), *Izvestiya Vysshikh Uchebnykh Zavedenii. Pishchevaya Tekhnologiya (News of Institutes of Higher Education. Food Technology)*, 1988, no. 1, pp.89-97.
5. Ivanets, V.N. and Poznyakovskii, V.M., *Gigienicheskie aspekty, tekhnologiya, i apparaturnoe oformlenie vitaminizatsii pishchevykh produktov (Hygienic Aspects, Technology, and Equipment Implementation of Food Product*

Vitaminization), Kemerovo: KemTIPP, 1991.

6. Ivanets, V.N. and Fedosenkov, B.A., *Protsessy dozirovaniya sypuchikh materialov v smeseprigotovitel'nykh agregatakh nepreryvnogo deistviya: obobshchennaya teoriya i analiz* (Bulk Material Dosing Processes in Continuous Mixture Preparing Units: Generalized Theory and Analysis), Kemerovo: KemTIPP, 2002.

7. Ivanets, V.N., Zhukov, A.N., and Borodulin, D.M., *Analiz chastotno-vremennykh kharakteristik smesitelya nepreryvnogo deistviya tsentrobezhnogo tipa* (Analysis of the time-and-frequency characteristics of a continuous centrifugal mixer), *Khranenie i Pererabotka Sel'khozsyrya* (Storage and Processing of Farm Products), 2004, no. 2, pp. 52-54.

8. Kafarov, V.V. and Dorokhov, I.N. *Sistemnyi analiz protsessov khimicheskoi Tekhnologii* (System Analysis of Chemical Engineering Processes), Moscow: Nauka, 1976.

9. Lazareva, T.Ya. and Martem'yanov, Yu.F., *Osnovy teorii avtomaticheskogo upravleniya. Uchebnoe posobie* (Foundations of Automatic Control Theory: Textbook), Tambov: Izd. Tambov. Gos. Univ., 2004.

10. Makarov, Yu.I., *Apparaty dlya smesheniya sypuchikh materialov* (Apparatuses for the Mixing of Bulk Materials), Moscow: Mashinostroenie, 1973.

11. RF Patent 2361653, *Byull. Izobret.*, 2009, no 20.

12. RF Patent 2207186, *Byull. Izobret.*, 2003, no. 18.

13. Dehling, H.G., Hoffmann, A.C., and Stuu, H.W., Stochastic models for transport in a fluidized bed, *SIAM Journal on Applied Mathematics*, 1999, vol. 60, no. 1, p. 337-358.

14. Hoffmann, A.C. and Paarhuis, H.I., A study of the particle residence time distribution in continuous fluidized beds, *Institution of Chemical Engineers Symposium Series*, 1990, vol. 121, p. 37-49.

15. Salahudeen, S.A. and AlOthman, O., Optimization of rotor speed based on stretching, efficiency, and viscous heating in nonintermeshing internal batch mixer: simulation and experimental verification, *Journal of Applied Polymer Science*, 2013, vol. 127, no. 4, pp. 2739-2748.

